

# MATHEMATICAL ENGINEERING TECHNICAL REPORTS

## Oscillation Pattern Analysis for Gene Regulatory Networks with Negative Cyclic Feedback

Yutaka HORI and Shinji HARA

(Communicated by Kazuo MUROTA)

METR 2010-29

October 2010

DEPARTMENT OF MATHEMATICAL INFORMATICS  
GRADUATE SCHOOL OF INFORMATION SCIENCE AND TECHNOLOGY  
THE UNIVERSITY OF TOKYO  
BUNKYO-KU, TOKYO 113-8656, JAPAN

**WWW page:** <http://www.keisu.t.u-tokyo.ac.jp/research/techrep/index.html>

The METR technical reports are published as a means to ensure timely dissemination of scholarly and technical work on a non-commercial basis. Copyright and all rights therein are maintained by the authors or by other copyright holders, notwithstanding that they have offered their works here electronically. It is understood that all persons copying this information will adhere to the terms and constraints invoked by each author's copyright. These works may not be reposted without the explicit permission of the copyright holder.

# Oscillation Pattern Analysis for Gene Regulatory Networks with Negative Cyclic Feedback

Yutaka HORI\*, and Shinji HARA†

October 5th, 2010

## Abstract

Negative cyclic feedback has been considered to be a core circuit to produce sustained oscillations in gene regulatory networks. In this paper, we investigate quantitative properties of the periodic oscillations observed in cyclic gene regulatory networks with negative feedback, and we provide analytic estimates of frequency, phase and amplitude. We employ the harmonic balance method, which is one of the frequency domain techniques to examine nonlinear oscillatory behaviors by approximating with bias and first order harmonic components. We then solve the harmonic balance equations by utilizing the structure of gene expression dynamics. The presented estimates are analytically written only in terms of essential biochemical parameters proposed in authors' previous work, and hence they can be easily applied to large-scale cyclic gene regulatory networks involving any number of genes. Our results are demonstrated with illustrative numerical examples, and some novel biological insights are presented.

## 1 INTRODUCTION

Oscillatory gene expression in gene regulatory networks has been receiving much attention in recent years, since it has begun to be understood that the periodic oscillations of the transcription proteins regulate rhythmic bodily functions, such as circadian rhythms [1]. Recently, it has been revealed that the period of the oscillations ranges from minutes to hours depending on the

---

\*Department of Information Physics and Computing, Graduate School of Information Science and Technology, The University of Tokyo, 7-3-1 Hongo, Bunkyo-ku, Tokyo 113-8656, Japan. E-mail: [Yutaka\\_Hori@ipc.i.u-tokyo.ac.jp](mailto:Yutaka_Hori@ipc.i.u-tokyo.ac.jp)

†Department of Information Physics and Computing, Graduate School of Information Science and Technology, The University of Tokyo, 7-3-1 Hongo, Bunkyo-ku, Tokyo 113-8656, Japan. E-mail: [Shinji\\_Hara@ipc.i.u-tokyo.ac.jp](mailto:Shinji_Hara@ipc.i.u-tokyo.ac.jp)

role of the transcription proteins [2], and that the phase of the oscillations also plays an important role in producing the circadian clock (see [1] and references therein). Thus, it is one of the interesting and essential problems to unravel the quantitative properties of the periodic oscillations observed in gene regulatory networks. Specifically, it is desirable to develop a unified analysis scheme that can investigate the relation between the biochemical parameters of gene regulatory networks and the oscillation profiles such as frequency, phase and amplitude of the periodic oscillations.

Although the network motifs of the existing gene regulatory networks in living organisms are complicated, it is known that a simple loop motif illustrated in Fig. 1, which we refer to as *cyclic feedback*, can also show the periodic oscillations of protein concentrations. In particular, it is interesting that recent theoretical study proved that the cyclic feedback structure plays a key role to produce sustained oscillations in gene regulatory networks, and the other interactions increase its robustness [3]. Therefore, better understanding of dynamical properties of cyclic gene regulatory networks becomes the first key step to reveal the whole picture of large-scale complicated gene regulatory networks.

One of the pioneering experimental studies of cyclic gene regulatory networks was performed in Elowitz and Leibler [4], where three repressor genes were artificially implemented in *Escherichia Coli* as shown in Fig. 1 (center) so that the resulting gene regulatory network exhibits periodic oscillations. Inspired by this work, Samad *et al.* [5] numerically examined oscillation frequency of the protein levels in the cyclic gene regulatory networks. The idea was based on Rapp [6], where a harmonic balance technique was applied to the Goodwin oscillator [7]. However, the phase of the oscillations, which is one of important factors in gene regulatory networks associated with circadian rhythms, was not argued in these works. Although qualitative relation of the phase of the oscillations and the regulatory network pattern was studied in [8], it is difficult to obtain general knowledge of oscillation profiles and biological insight from the numerical simulations presented in these previous works.

Hence, the objective of this paper is to *systematically* unravel the quantitative relation between the biochemical parameters and the profiles of oscillations in large-scale cyclic gene regulatory networks. Specifically, we obtain analytic estimates of frequency, phase and amplitude of periodic oscillations based on the harmonic balance method [9], which is one of the classical frequency domain techniques to examine nonlinear oscillatory behaviors by approximating the waveform with bias and first order harmonic components. In particular, we use the idea that the above estimation problem can be reduced to an eigenvalue/eigenvector problem [10], and we show that it can be greatly simplified by using the dynamical properties of the cyclic gene regulatory networks. The developed estimates have distinctive features that

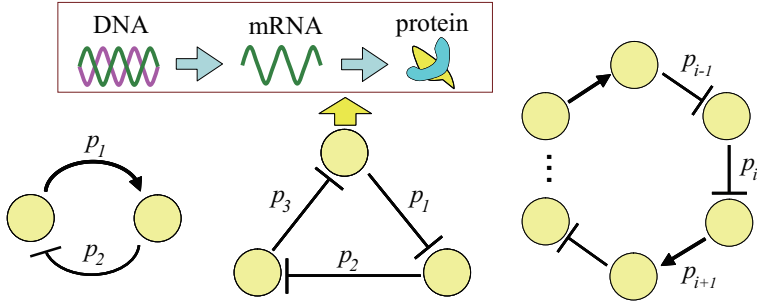


Figure 1: Gene regulatory networks with negative cyclic feedback. The symbols  $\rightarrow$  and  $\dashv$  represent activation and repression of transcription, respectively. (Left) activator-repressor motif, (Center) successive repressor motif or Repressilator motif [4], (Right) generic negative cyclic motif considered in this paper.

(i) they can be applied to gene regulatory networks consisting any number of genes, and (ii) they are expressed in analytic form. Thus, we can easily gain quantitative insights on the oscillation profiles.

This paper is organized as follows. In Section 2, the dynamical model of the cyclic gene regulatory networks is introduced. Section 3 formulates a framework for estimating the oscillation profiles by using multivariable harmonic balance. In Section 4, the oscillation profiles are analytically derived, and we will demonstrate our main results with an illustrative example and give novel biological insights based on the main results in Section 5. Section 6 is devoted to discuss the accuracy of our estimation. Finally, Section 7 concludes this paper.

## 2 Model description and Existence of Periodic oscillations

### 2.1 Modeling of cyclic gene regulatory networks

The gene regulatory networks where each protein activates or represses another transcription in a cyclic way as illustrated in Fig. 1, are called *cyclic* gene regulatory networks. The dynamics of mRNA and protein concentrations in the cyclic gene regulatory networks consisting of  $N$  genes is modeled as, for  $i = 1, 2, \dots, N$ ,

$$\begin{aligned} \dot{r}_i(t) &= -a_i r_i(t) + \beta_i f_i(p_{i-1}(t)), \\ \dot{p}_i(t) &= c_i r_i(t) - b_i p_i(t), \end{aligned} \quad (1)$$

where  $r_i \in \mathbb{R}_+ (:= \{x \in \mathbb{R} \mid x \geq 0\})$  and  $p_i \in \mathbb{R}_+$  denote the normalized concentrations of the  $i$ -th mRNA and its corresponding protein synthesized

in the  $i$ -th gene, respectively [4, 5]<sup>1</sup>. Let  $p_0(t) := p_N(t)$  and  $r_0(t) := r_N(t)$  for the sake of notational simplification. Positive constants  $a_i, b_i, c_i$  and  $\beta_i$  represent the followings:  $a_i$  and  $b_i$  denote the degradation rates of the  $i$ -th mRNA and protein, respectively;  $c_i$  and  $\beta_i$  denote the translation and transcription rates, respectively. A monotonic function  $f_i(\cdot) : \mathbb{R}_+ \rightarrow \mathbb{R}_+$  represents either activation or repression of the transcription: it is defined for repression as  $f_i(0) = 1$  and  $f_i(\infty) = 0$  (monotonically decreasing), whereas for activation as  $f_i(0) = 0$  and  $f_i(\infty) = 1$  (monotonically increasing). In practical applications, the following Hill function is often introduced to describe biochemical characterization:

$$f_i(p_{i-1}) = \begin{cases} \frac{1}{1+p_{i-1}^\nu} (=F_R(p_{i-1})) & \text{(for repression)} \\ \frac{p_{i-1}^\nu}{1+p_{i-1}^\nu} (=F_A(p_{i-1})) & \text{(for activation)} \end{cases} \quad (2)$$

where  $\nu(\geq 1) \in \mathbb{R}_+$  is the Hill coefficient, which represents a degree of cooperative binding, and determines the nonlinearity of the system [11].

Suppose  $a_1 = a_2 = \dots = a_N$  and  $b_1 = b_2 = \dots = b_N$  in (1). Then, the overall dynamics of gene regulatory network systems defined by (1) can be formulated as shown in Fig. 2(Left), where

$$h(s) := \frac{1}{(T_a s + 1)(T_b s + 1)}, \quad T_a := \frac{1}{a}, \quad T_b := \frac{1}{b}, \quad (3)$$

and  $\mathbf{f}$  is a static vector nonlinearity function defined by

$$\mathbf{f} := [R_1^2 f_1(\cdot), R_2^2 f_2(\cdot), \dots, R_N^2 f_N(\cdot)]^T \quad (4)$$

with

$$R_i := \frac{\sqrt{c_i \beta_i}}{\sqrt{ab}}. \quad (i = 1, 2, \dots, N). \quad (5)$$

Note that  $R_i$  is a dimensionless physical quantity that expresses the ratio between geometric means of degradation and production rates, and has been proposed as one of the dominant parameters which determine the existence of periodic oscillations [12].

## 2.2 Existence of periodic oscillations

Let  $\delta$  be defined as

$$\delta := \left( \frac{df_1}{dp} \right) \cdot \left( \frac{df_2}{dp} \right) \cdots \left( \frac{df_N}{dp} \right). \quad (6)$$

---

<sup>1</sup> $r_i$  and  $p_i$  are normalized by activation/repression coefficient in the Hill function, and dimensionless quantities.

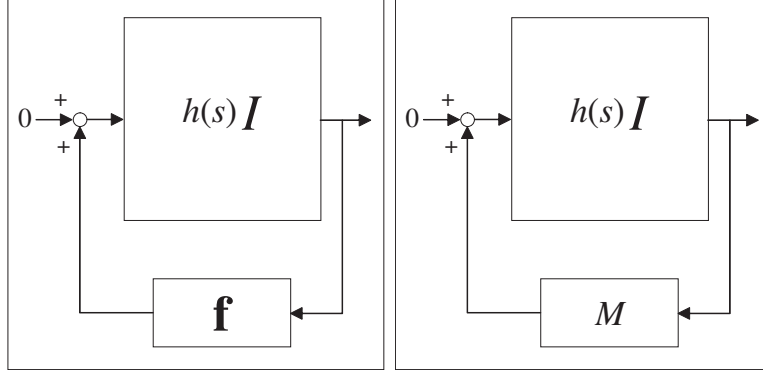


Figure 2: (Left) Block diagram of negative cyclic gene regulatory networks, (Right) Linearized system around an equilibrium

It has been shown that almost all solutions of (1) asymptotically converge to one of equilibria when  $\delta > 0$  [5, 13], while the protein concentrations exhibit oscillatory behaviors as well as convergence when  $\delta < 0$ . Therefore, we focus on the class of cyclic gene regulatory networks that satisfy the following assumption in this paper.

**Assumption 1.** For given  $f_i(\cdot)$  ( $i = 1, 2, \dots, N$ ),  $\delta < 0$ .

This assumption implies that there is an odd number of repressive interactions ( $df_i/dp < 0$ ) between genes, and such feedback structure is referred to as *negative cyclic feedback* in this paper.

Next, we briefly review the graphical and analytic criteria for the existence of periodic oscillations of protein concentrations in cyclic gene regulatory networks [12]. Let  $\mathcal{G}(s)$  denote a linearized system of (1) at an equilibrium state. It is clear from Fig. 2(Left) that  $\mathcal{G}(s) := (\phi(s)I - M)^{-1}$  as depicted in Fig. 2(Right), where

$$\phi(s) := \frac{1}{h(s)}, M := \text{cyc}(R_1^2 \zeta_1, R_2^2 \zeta_2, \dots, R_N^2 \zeta_N) \in \mathbb{R}^{N \times N} \quad (7)$$

, and  $\zeta_i := f'_i(p_{i-1}^*)$  is a linearized gain of  $f_i(\cdot)$  at the equilibrium state  $p_i^*$  ( $i = 1, 2, \dots, N$ ).  $\text{cyc}(\cdot)$  is defined as

$$\text{cyc}(z_1, z_2, \dots, z_N) := \begin{bmatrix} 0 & 0 & 0 & \cdots & z_1 \\ z_2 & 0 & 0 & \ddots & 0 \\ 0 & z_3 & 0 & \ddots & \vdots \\ \vdots & \ddots & \ddots & \ddots & \vdots \\ 0 & \cdots & 0 & z_N & 0 \end{bmatrix}. \quad (8)$$

It has been shown [12] that the equilibrium state of the system (1) is unique, and the existence of periodic oscillations is guaranteed if the unique equilibrium state is locally unstable, because Poincaré-Bendixson type theorem [14]

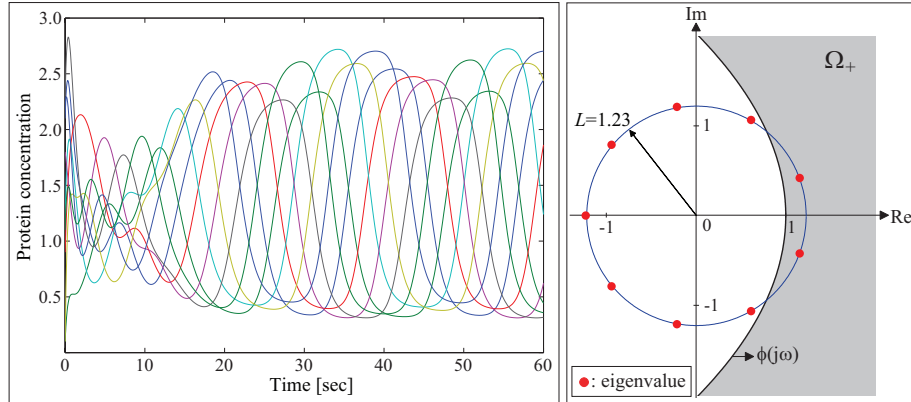


Figure 3: (Left) Time plot of oscillatory protein concentrations, (Right) graphical criterion for the existence of periodic oscillations [12].

holds for the cyclic gene regulatory network system. The following proposition gives a graphical criterion for the existence of periodic oscillations in the cyclic gene regulatory networks.

**Proposition 1.** [12] *Consider the cyclic gene regulatory network systems modeled by (1), and the linear system  $\mathcal{G}(s)$ . Then, the system has periodic oscillations of protein concentrations  $p_i(t)$  ( $i = 1, 2, \dots, N$ ) if at least one of the eigenvalues of  $M$  lies inside the domain  $\Omega_+$  defined by*

$$\Omega_+ := \phi(\mathbb{C}_+) = \{\lambda \in \mathbb{C} \mid \exists s \in \mathbb{C}_+ \text{ s.t. } \phi(s) = \lambda\}. \quad (9)$$

An example of the region  $\Omega_+$  and the eigenvalues of  $M$  is depicted in Fig. 3(Right). The above theorem allows us to check the existence of periodic oscillations easily even if the degree of the linearized gene regulatory network systems  $\mathcal{G}(s)$  is large, because the region  $\Omega_+$  is determined from the simple second-order polynomial  $\phi(s) = (T_a s + 1)(T_b s + 1)$  and the size of the matrix  $M$  is relatively small compared to the degree of the overall system  $\mathcal{G}(s)$ . Note that the above graphical condition is necessary and sufficient for instability of the linearized system  $\mathcal{G}(s)$  (see [15] for details).

Moreover, analytic criteria for the existence of periodic oscillations have been obtained based on the simple graphical criterion. In particular, it has been shown [12] that

$$Q := \frac{\sqrt{T_a T_b}}{(T_a + T_b)/2} \quad (10)$$

is also another dominant physical quantities that determine the existence of periodic oscillations. It is a dimensionless parameter expressing the ratio between arithmetic and geometric means of mRNA and protein degradation

rates, and satisfies  $0 < Q \leq 1$ . Thus, it can be a measure of difference between degradation time constants of mRNA and protein, because it gets close to unity as  $T_a$  and  $T_b$  get closer.

In summary, the existence of periodic oscillations in cyclic gene regulatory networks is determined by the parameters  $(N, \nu, Q, R_\ell)$  ( $\ell = 1, 2, \dots, N$ ). Therefore, these parameters have been considered as essential physical quantities for the existence of periodic oscillations [12].

In the following, we assume the existence of periodic oscillations and investigate oscillation profiles of protein levels in large-scale negative cyclic gene regulatory networks. The problem considered in this paper can be summarized as follows.

**Problem.** *For large-scale negative cyclic gene regulatory networks modeled by (1), derive analytic estimates of frequency, phase and amplitude of oscillatory protein concentrations  $p_i(t)$  ( $i = 1, 2, \dots, N$ ). Then, find biological insight into the relation between biochemical parameters and the oscillation profiles.*

### 3 Oscillation Pattern analysis based on Multivariable Harmonic Balance

In this section, we provide a framework of estimating the oscillation profiles. We first derive quasi-linear systems of (1) by approximating the oscillatory waveform of protein levels  $p_i(t)$  and the nonlinearity  $f_i(\cdot)$  ( $i = 1, 2, \dots, N$ ) of the system, then analyze the oscillation profile based on the approximation.

Let the waveform of  $p_i(t)$  be approximated by

$$p_i(t) \simeq x_i + y_i \sin(\varpi t + \varphi_i) \quad (i = 1, 2, \dots, N), \quad (11)$$

where  $x_i > 0$  and  $y_i > 0$  denote the bias and the amplitude of the first order harmonic components of the  $i$ -th protein, respectively, and  $\varphi_i$  is the relative phase of the  $i$ -th protein. Throughout this paper, we define  $\varphi_1 := 0$  without loss of generality. Then, the nonlinear function  $f_i(p_{i-1}(t))$  can be approximated by its describing functions [9]

$$\eta_i(x_{i-1}, y_{i-1}) := \frac{R_i^2}{2\pi x_{i-1}} \int_{-\pi}^{\pi} f_i(x_{i-1} + y_{i-1} \sin(t)) dt. \quad (12)$$

and

$$\xi_i(x_{i-1}, y_{i-1}) := \frac{R_i^2}{\pi y_{i-1}} \int_{-\pi}^{\pi} f_i(x_{i-1} + y_{i-1} \sin(t)) \sin(t) dt \quad (13)$$

The describing functions  $\eta_i(x_{i-1}, y_{i-1})$  and  $\xi_i(x_{i-1}, y_{i-1})$  represent the gains of  $R_i^2 f_i(\cdot)$  for the bias and the harmonic component, respectively, when the input is the biased sinusoidal of  $x_{i-1} + y_{i-1} \sin(\varpi t)$ .

Consequently, the closed loop equations that  $\mathbf{x}$  and  $\mathbf{y}$  are expected to satisfy for the quasi-linear system are obtained as

$$\begin{aligned} (I - h(0)\mathcal{K}_0(\mathbf{x}, |\mathbf{y}|)) \mathbf{x} &= 0, \\ (I - h(j\varpi)\mathcal{K}_1(\mathbf{x}, |\mathbf{y}|)) \mathbf{y} &= 0, \end{aligned} \quad (14)$$

where  $\mathcal{K}_0(\mathbf{x}, |\mathbf{y}|) := \text{cyc}(\eta_1, \eta_2, \dots, \eta_N)$ ,  $\mathcal{K}_1(\mathbf{x}, |\mathbf{y}|) := \text{cyc}(\xi_1, \xi_2, \dots, \xi_N)$ ,  $\mathbf{x} := [x_1, x_2, \dots, x_N]^T \in \mathbb{R}_+^N$  and  $\mathbf{y} := [y_1 e^{j\varphi_1}, y_2 e^{j\varphi_2}, \dots, y_N e^{j\varphi_N}]^T \in \mathbb{C}^N$ .  $|\mathbf{y}|$  is defined as an elementwise absolute value, thus  $|\mathbf{y}| = [y_1, y_2, \dots, y_N]^T \in \mathbb{R}_+^N$ . Therefore, the oscillation profile analysis reduces to the problem of finding  $3N$  variables  $(\varpi, x_1, x_2, \dots, x_N, y_1, y_2, \dots, y_N, \varphi_1, \varphi_2, \dots, \varphi_N)$ , or  $(\varpi, \mathbf{x}, \mathbf{y})$ , satisfying (14). Note that the first and second equations in (14) are referred to as *bias* and *harmonic balance equations*, respectively.

Let  $\mathbf{x}^*$  and  $\mathbf{y}^*$  denote the constant vectors that simultaneously satisfy the bias and harmonic balance equations in (14). Define the linear systems  $\mathcal{H}_0(s)$  and  $\mathcal{H}_1(s)$  as

$$\mathcal{H}_\bullet(s) := (\phi(s)I - K_\bullet)^{-1} \quad (\bullet = 0, 1), \quad (15)$$

where  $K_\bullet$  is the constant matrices defined by  $K_\bullet := \mathcal{K}_\bullet(\mathbf{x}^*, |\mathbf{y}^*|)$  ( $\bullet = 0, 1$ ). The systems  $\mathcal{H}_\bullet(s)$  ( $\bullet = 0, 1$ ) are obtained by replacing the nonlinearity  $f_i(\cdot)$  with the constant gain computed from the describing functions. Thus, the associated linear system  $\mathcal{H}_\bullet(s)$  contains some information on the oscillations of the original nonlinear system. According to Iwasaki [10], the predicted oscillation  $(\varpi, \mathbf{x}^*, \mathbf{y}^*)$  is expected stable if both  $\mathcal{H}_0(s)$  and  $\mathcal{H}_1(s)$  are marginally stable with the poles of  $s = 0$  and  $s = \pm j\varpi$  on the imaginary axis, and the rest in the open left half plane, respectively. Therefore, the problem of oscillation profile analysis addressed in Section 2.2 can be reduced to the following proposition.

**Proposition 2.** *Consider the gene regulatory networks modeled by (1). Suppose there exist  $(\varpi, \mathbf{x}, \mathbf{y})$  satisfying (14). Then, the oscillatory protein concentrations  $p_i(t)$  are expected at frequency  $\varpi$ , with phase  $\varphi_i$ , bias  $x_i$  and amplitude  $y_i$ , i.e.*

$$p_i(t) \simeq x_i + y_i \sin(\varpi t + \varphi_i) \quad (16)$$

for  $i = 1, 2, \dots, N$ , where  $\varpi, \varphi_i, x_i$  and  $y_i$  satisfy both of the following conditions: (i) (14) is satisfied, and (ii)  $\mathcal{H}_\bullet(s)$  ( $\bullet = 0, 1$ ) are marginally stable.

It should be noted that existence of the solution  $(\varpi, \mathbf{x}, \mathbf{y})$  which satisfies (14) is plausible when the waveform of the oscillations is sufficiently similar to the biased sinusoidal of (11). For the sake of analysis, we hereafter assume the existence of a solution in the bias and harmonic balance equations.

**Assumption 2.** *There exist  $\varpi, \mathbf{x}$  and  $\mathbf{y}$  which satisfy both bias and harmonic balance equations in (14) simultaneously.*

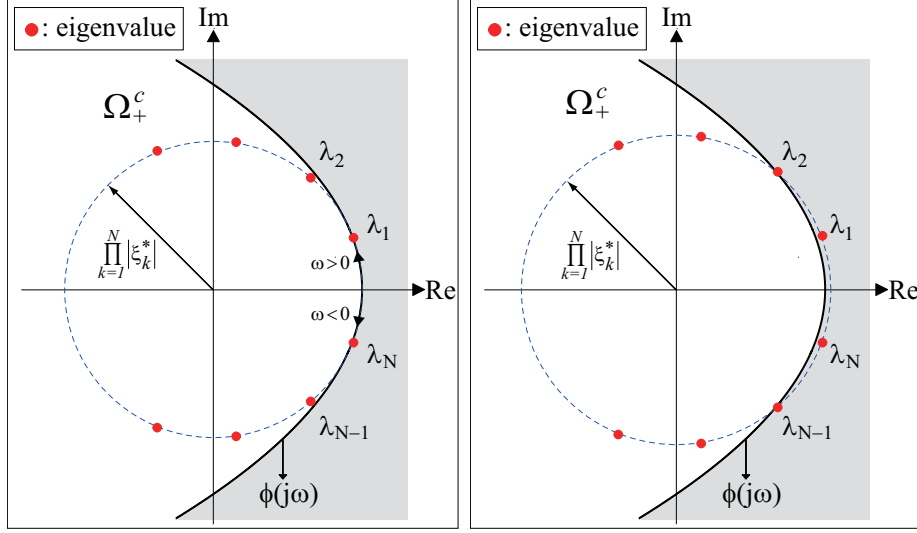


Figure 4: Graphical interpretation of the harmonic balance equation: (Left)  $\phi(j\varpi) = \lambda_1$  and  $\phi(j\varpi) = \lambda_N$ , and the marginal stability condition in Proposition 2 is satisfied. (Right)  $\phi(j\varpi) = \lambda_2$  and  $\phi(j\varpi) = \lambda_{N-1}$ , but the marginal stability condition is not satisfied.

It has been pointed out in Iwasaki [10] that the problem of solving the bias and harmonic balance equations is essentially reduced to an eigenvalue/eigenvector problem. The idea is as follows. First, we have

$$\begin{aligned} (\phi(0)I - \mathcal{K}_0(\mathbf{x}, |\mathbf{y}|))\mathbf{x} &= 0, \\ (\phi(j\varpi)I - \mathcal{K}_1(\mathbf{x}, |\mathbf{y}|))\mathbf{y} &= 0, \end{aligned} \quad (17)$$

by dividing the bias and harmonic balance equations by  $h(0)$  and  $h(j\varpi)$ , respectively. Then,  $\phi(0)$  and  $\phi(j\varpi)$  can be regarded as eigenvalues, and  $\mathbf{x}$  and  $\mathbf{y}$  as eigenvectors of the matrices  $\mathcal{K}_0$  and  $\mathcal{K}_1$ , respectively. Thus, the problem is reduced to compute the eigenvalue/eigenvector of the matrices  $\mathcal{K}_0$  and  $\mathcal{K}_1$ . However, the above eigenvalue/eigenvector problem is not straightforward, because  $\mathcal{K}_0$  and  $\mathcal{K}_1$  actually depend on  $\mathbf{x}$  and  $\mathbf{y}$ . Nevertheless, this view is helpful in our analysis.

In the next section, we will derive analytic forms of estimating the oscillation profiles based on the above observation.

## 4 Main result

In this section, we solve the bias and the harmonic balance equations, and analytically derive profiles of the oscillatory protein concentrations in terms of the biological parameters. It is assumed in this section that the system (1)

has an oscillatory solution, and the bias and the harmonic balance equations have the solution  $(\varpi, \mathbf{x}, \mathbf{y})$  that satisfies both (i) and (ii) in Proposition 2.

#### 4.1 Estimation of frequency

We here derive an analytic expression of the oscillation frequency  $\varpi$  based on a graphical interpretation of (17). It follows from (17) that  $\varpi$  satisfies  $\phi(j\varpi) = \lambda_i$  for some  $\lambda_i$  ( $i = 1, 2, \dots, N$ ), which is the eigenvalue of the matrix  $K_1$ . This means that the mapping  $\phi(j\omega)$  over  $\omega \in (-\infty, \infty)$  passes one of the eigenvalues of  $K_1$  at the estimated frequency  $\varpi$ . Using the cyclic structure of  $K_1$ , we see that the eigenvalues of  $K_1$  becomes

$$\lambda_i := \left| \prod_{k=1}^N \xi_k^* \right|^{\frac{1}{N}} e^{j \frac{2i-1}{N} \pi} \quad (i = 1, 2, \dots, N) \quad (18)$$

with  $\xi_k^* := \xi_k(x_{k-1}^*, y_{k-1}^*)$ . It is clear from (18) that the eigenvalues are uniformly located on a circle with a center at the origin and radius of  $\prod_{k=1}^N |\xi_k^*|^{1/N}$  as shown in Fig. 4.

Since the solution  $(\mathbf{x}^*, \mathbf{y}^*)$  of (14) is not unique in general and the eigenvalues of  $K_1$  may vary depending on  $(\mathbf{x}^*, \mathbf{y}^*)$ , there can be multiple candidates of oscillation profile  $(\varpi, \mathbf{x}^*, \mathbf{y}^*)$ , which satisfies the bias/harmonic balance equations, as illustrated in Fig. 4. The most likely frequency of oscillations are then obtained by the marginal stability condition in Proposition 2. In particular, the marginal stability of  $\mathcal{H}_\bullet(s)$  can be easily determined by the following lemma (see Appendix A for the proof).

**Lemma 1.** The system  $\mathcal{H}_\bullet(s)$  ( $\bullet = 0, 1$ ) defined by (15) has at least one pole on the imaginary axis, and the rest in the open left half plane if and only if at least one eigenvalue of  $K_\bullet$  lies on the curve  $\{\phi(j\omega) \mid \omega \in \mathbb{R}\}$ , and the rest lies inside the open set  $\Omega_+^c$ , where  $\Omega_+^c := \{\gamma \in \mathbb{C} \mid \phi(s) \neq \gamma \text{ for } \forall s \in \mathbb{C}_+\}$ .

An example is shown in Fig. 4, where the left figure implies marginal stability of  $\mathcal{H}_1(s)$ , but the right does not. From these arguments, we have the following analytic estimate of frequency of periodic oscillations in negative cyclic gene regulatory networks (see Appendix B for the rigorous proof).

**Theorem 1.** Consider the cyclic gene regulatory networks modeled by (1). Then, the frequency  $\varpi$  of oscillatory protein concentrations is expected as

$$\varpi = \frac{-1 + \sqrt{1 + Q^2 \tan^2(\frac{\pi}{N})}}{Q \tan(\frac{\pi}{N})} \frac{1}{T_G}, \quad (19)$$

where  $T_G := \sqrt{T_a T_b}$ .

This theorem gives an expected frequency of oscillations in cyclic gene regulatory networks composed of any number of genes. Since the estimated

frequency is written only in terms of the kinetic parameters of the system, namely  $N, Q$  and  $T_G$ , we can easily compute it for large-scale cyclic gene regulatory networks, and we reveal the relation between the parameters and the frequency. It should be noted that this result is consistent with the statement presented in [5] that  $\varpi$  is in inverse proportion to the degradation time constants. It is, however, fair to note that actual oscillation frequency may somewhat differ from the above estimate, because our analysis is based on the approximation of (11). Discussion on the accuracy of the estimated values can be found in Section 6.

## 4.2 Estimation of phase

Next, we consider the phase  $(\varphi_2, \varphi_3, \dots, \varphi_N)$  of the oscillations, and derive analytic estimates by computing the eigenvector  $\mathbf{y}$  in (17). Note again that  $\varphi_1 := 0$  without loss of generality.

Let us first consider a simple case. Suppose

$$c_1 = c_2 = \dots = c_N, \beta_1 = \beta_2 = \dots = \beta_N \quad (20)$$

and all the interactions are repressive, *i.e.*,  $f_1(\cdot) = f_2(\cdot) = \dots = f_N(\cdot) = F_R(\cdot)$ . Then, the dynamical model in (1) becomes symmetric in that the dynamics is not affected by replacing the gene's index  $i$ . It implies that  $x_1 = x_2 = \dots = x_N$  and  $y_1 = y_2 = y_3 = \dots = y_N$ , and only the phase of the proteins is different between each other. Thus, the matrices  $K_\bullet$  ( $\bullet = 0, 1$ ) belong to a class of circulant matrices, since  $\xi_1(x_N, y_N) = \xi_2(x_1, y_1) = \dots = \xi_N(x_{N-1}, y_{N-1})$  holds. Therefore,  $K_1$  is diagonalized with the discrete Fourier transform matrix

$$\mathcal{F} := \frac{1}{\sqrt{N}} \begin{bmatrix} 1 & 1 & 1 & \dots & 1 \\ 1 & e^{-\frac{2j\pi}{N}} & e^{-\frac{4j\pi}{N}} & \dots & e^{-\frac{2j(N-1)\pi}{N}} \\ 1 & e^{-\frac{4j\pi}{N}} & e^{-\frac{8j\pi}{N}} & \dots & e^{-\frac{4j(N-1)\pi}{N}} \\ \vdots & \vdots & \vdots & \ddots & \vdots \\ 1 & e^{-\frac{2j(N-1)\pi}{N}} & e^{-\frac{4j(N-1)\pi}{N}} & \dots & e^{-\frac{2j(N-1)^2\pi}{N}} \end{bmatrix}, \quad (21)$$

which is unitary [16]. In particular, the corresponding eigenvector to  $\lambda_1 (= \phi(j\varpi))$  in (18) is obtained as

$$\mathbf{v} := [1, e^{\frac{j(N-1)\pi}{N}}, e^{\frac{2j(N-1)\pi}{N}}, \dots, e^{\frac{j(N-1)^2\pi}{N}}]^T \in \mathbb{C}^N. \quad (22)$$

Note that the expected frequency  $\varpi$  necessarily satisfies  $\phi(j\varpi) = \lambda_i$  with  $i = 1$  (see the proof of Theorem 1 in Appendix B). Hence, the expected phase is obtained as follows.

**Proposition 3.** *Consider the cyclic gene regulatory networks modeled by (1). Suppose (20) holds and all the interactions between genes are repressive,*

i.e.,  $f_1(\cdot) = f_2(\cdot) = \dots = f_N(\cdot) = F_R(\cdot)$ . Then, the phase  $\varphi_i$  is expected as

$$\varphi_i = \frac{(i-1)(N-1)\pi}{N} \quad (i = 2, 3, \dots, N). \quad (23)$$

It follows from (23) that  $\varphi_{i+1} - \varphi_i = (1 - 1/N)\pi$ , and we see that the phase of oscillations is expected to uniformly distribute over  $2\pi$ .

Next, we consider an analytic estimate of phase of oscillations for the *asymmetric* case where (20) is not assumed. Since the matrix  $K_1$  is no longer circulant in this case, the eigenvector which corresponds to  $\lambda_1 (= \phi(j\varpi))$  is different from  $\mathbf{v}$ .

Then, our approach is to find the similarity transformation matrix which reduces  $K_1$  to a circulant matrix, and obtain the phasor  $\mathbf{y}$  by using the transformation matrix and  $\mathbf{v}$ . The following lemma is a key to obtain our analytic result.

**Lemma 2.** Consider a constant matrix  $K_1 := \mathcal{K}_1(\mathbf{x}^*, |\mathbf{y}^*|) \in \mathbb{R}^{N \times N}$ . Then, there exists a diagonal matrix  $D := \text{diag}(d_1, d_2, \dots, d_N) \in \mathbb{C}^{N \times N}$  that diagonalizes  $K_1$  via

$$\mathcal{F}^{-1} D^{-1} K_1 D \mathcal{F} = \text{diag}(\lambda_1, \lambda_2, \dots, \lambda_N), \quad (24)$$

where  $\lambda_i$  ( $i = 1, 2, \dots, N$ ) is defined by (18) and  $\mathcal{F}$  is the discrete Fourier transform matrix defined by (21). In particular, the diagonal matrix  $D$  can be determined as

$$d_i = \frac{\prod_{k=1}^i \xi_k^*}{\prod_{k=1}^N |\xi_k^*|^{\frac{i-1}{N}}} e^{-\frac{ji\pi}{N}} \quad (i = 1, 2, \dots, N). \quad (25)$$

From this lemma, we see that  $K_1$  can be transformed to a circulant matrix via similarity transformation  $D^{-1} K_1 D$ , and thus, the corresponding eigenvector  $\mathbf{y}^*$  to  $\lambda_1 (= \phi(j\varpi))$  is obtained as  $\mathbf{y}^* = D\mathbf{v}$ . This observation immediately leads to the following analytic estimate of phase for large-scale negative cyclic gene regulatory networks.

**Theorem 2.** Consider the cyclic gene regulatory networks modeled by (1). Then, the phase shift  $(\varphi_{i+1} - \varphi_i)$  between the  $i+1$ -th and the  $i$ -th protein is expected as

$$\varphi_{i+1} - \varphi_i = \left( Z - \frac{1}{N} \right) \pi \quad (26)$$

for  $i = 1, 2, \dots, N$ , where

$$Z = \begin{cases} 1 & \text{if } f_{i+1}(\cdot) = F_R(\cdot) \\ 0 & \text{if } f_{i+1}(\cdot) = F_A(\cdot) \end{cases}. \quad (27)$$

This theorem provides expected phase differences between oscillatory proteins. In particular, it is analytically written only in terms of biochemical parameters, and it can be applied to cyclic gene regulatory networks consisting of any number of genes. Thus, we can easily obtain biological insights as will be shown in Section 5.2. Note that the symmetric case considered in Proposition 3 corresponds to  $Z = 1$  for all  $i = 1, 2, \dots, N$ .

### 4.3 Estimation of bias and amplitude

We next estimate bias and amplitude of oscillations by finding  $\mathbf{x}$  and  $|\mathbf{y}|$  which satisfy both of the bias and harmonic balance equations given by (17).

Recall that the trajectory of the mapping  $\phi(j\omega)$  passes one of the eigenvalues of  $K_1$  at the estimated frequency  $\varpi$ , and the eigenvalues are distributed on a circle as was seen in (18). Thus, it follows that the solution  $\mathbf{x}^*$  and  $\mathbf{y}^*$  of both bias and harmonic balance equations satisfy

$$\left| \prod_{i=1}^N \xi_i(x_{i-1}, y_{i-1}) \right|^{\frac{1}{N}} = |\phi(j\varpi)|. \quad (28)$$

Note that the estimated frequency  $\varpi$  is independently determined regardless of  $\mathbf{x}^*$  and  $\mathbf{y}^*$ , because  $\mathbf{x}^*$  and  $\mathbf{y}^*$  exclusively affect the radius of the circle where the eigenvalues of  $K_1$  are located as shown in (18). Thus, the right-hand side of (28) is independent on  $x_i$  and  $y_i$  ( $i = 1, 2, \dots, N$ ), and is determined by (19).

Regarding the bias balance equation, we see from the similar argument to Section 4.1 that one of the eigenvalues of  $\mathcal{K}_0(\mathbf{x}, |\mathbf{y}|)$  should be located at  $\phi(0)(= 1)$  when the bias balance equation is satisfied. In particular, the eigenvalues  $\mu_i$  ( $i = 1, 2, \dots, N$ ) of  $K_0(= \mathcal{K}_0(\mathbf{x}^*, |\mathbf{y}^*|))$  are computed as  $\mu_i = (\prod_{i=1}^N \eta_i(x_{i-1}, y_{i-1}))^{\frac{1}{N}} e^{\frac{2ji\pi}{N}}$ , and are distributed on a circle. Thus, the equation which  $\mathbf{x}^*$  and  $\mathbf{y}^*$  should satisfy is obtained as  $\mu_N = \phi(0)$ , *i.e.*,

$$\left( \prod_{i=1}^N \eta_i(x_{i-1}, y_{i-1}) \right)^{\frac{1}{N}} = 1. \quad (29)$$

Consequently, we have the following proposition.

**Proposition 4.** *Consider the gene regulatory networks modeled by (1). Then, the expected bias  $\mathbf{x}$  and amplitude  $|\mathbf{y}|$  of periodic oscillations of oscillatory protein concentrations  $p_i(t)$  ( $i = 1, 2, \dots, N$ ) is expected to satisfy both (28) and (29) simultaneously.*

This proposition gives the equations that the expected bias and amplitude of oscillations should satisfy. Therefore, the amplitude of oscillations may be

obtained by numerically searching the solution of (28) and (29). However, no analytic solution has been obtained, and to get an analytic solution is one of our future works. Also, uniqueness of the solution has not been proven for (28) and (29). Thus, further study is required to obtain a reliable estimate of amplitude.

## 5 Numerical examples and Biological insight

In this section, we first show the distinctive features of our results with an illustrative numerical example, and then, present biological insights obtained from Theorem 1 and 2.

### 5.1 Numerical examples

Here, we examine the gene regulatory network where  $N = 6$  genes are involved as depicted in Fig. 5(Left). It means that  $f_1(\cdot) = f_4(\cdot) = f_6(\cdot) = F_R(\cdot)$  and  $f_2(\cdot) = f_3(\cdot) = f_5(\cdot) = F_A(\cdot)$  in (1). Suppose the kinetic parameters of gene expression are given by

$$\begin{aligned} a_1 = a_2 = \dots = a_6 = 1.0, b_1 = b_2 = \dots = b_6 = 3.0 \\ c_1 = c_3 = c_4 = c_6 = 3.2, c_2 = 2.8, c_5 = 3.7 \\ \beta_1 = \beta_4 = \beta_5 = 2.1, \beta_2 = \beta_3 = 2.9, \beta_6 = 3.1, \end{aligned}$$

and  $\nu = 2.8$ . The existence of periodic oscillations can be confirmed by the graphical criterion presented in Proposition 1, since two eigenvalues lie inside the region  $\Omega_+$  defined by (9).

Now, we investigate frequency of the periodic oscillations. The values of  $Q$  and  $T_G$  can be easily obtained as  $Q = 0.866$  and  $T_G = 0.577$  from the above parameters. Therefore, the expected frequency is obtained from (19) as

$$(\text{Estimated frequency } \varpi) = 0.409 \text{ [rad/s]}. \quad (30)$$

The actual frequency is computed as

$$(\text{Actual frequency}) = 0.428 \text{ [rad/s]} \quad (31)$$

by numerical simulation of (1) shown in Fig. 6. Thus, it is concluded that (19) approximates the actual frequency of the periodic oscillations with relative error of  $-4.44\%$ .

We next examine the phase shift between protein levels. It follows from Theorem 2 that the phase is determined from the number of genes,  $N$ , involved in gene regulatory networks and the activation-repression patterns of gene expression in Fig. 5(Left). The table below shows the estimated and

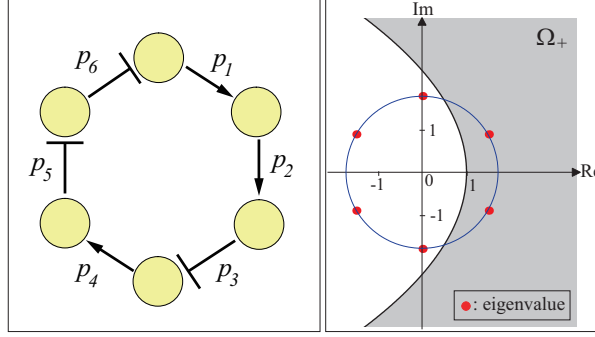


Figure 5: (Left) network motif of the considered negative cyclic gene regulatory network, (Right) graphical criterion for the existence of periodic oscillations (Proposition 1).

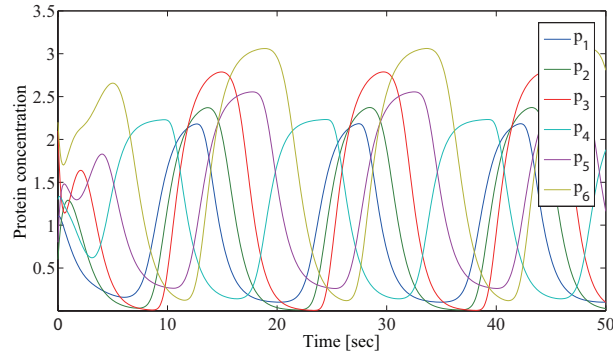


Figure 6: Time plot of oscillatory protein concentrations ( $(\prod_{i=1}^6 R_i^2)^{1/6} = 2.67$ ).

actual phase of protein concentrations, where phase of  $p_1(t)$  is set to zero, *i.e.*,  $\varphi_1 = 0$ .

Protein	$p_2$	$p_3$	$p_4$	$p_5$	$p_6$
Estimated [deg]	330.0	300.0	90.0	60.0	210.0
Actual [deg]	333.1	303.7	93.1	63.7	213.2

The table indicates that the actual phase shift is approximated by (26) with high precision.

Note that our estimation can also be easily applied to the existing synthetic biological oscillator named Repressilator, which was implemented in *Escherichia coli* with a cyclic network motif as illustrated in Fig. 1 (Center) [4].

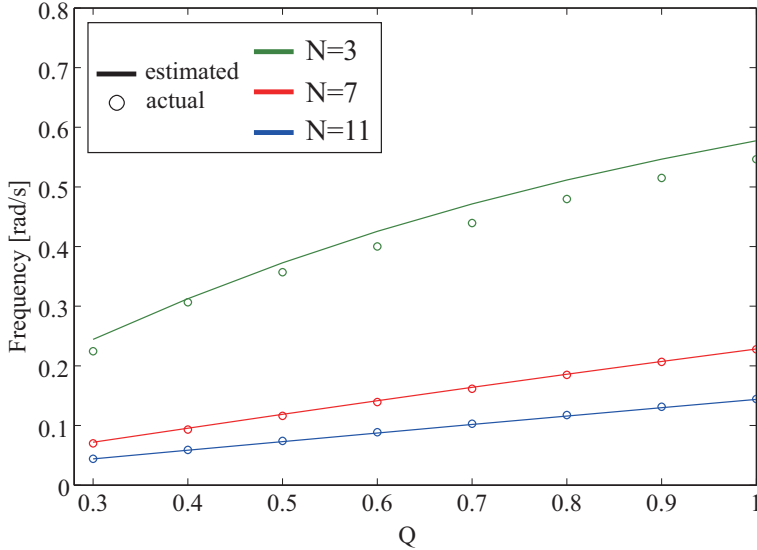


Figure 7: Estimated and actual frequency of protein concentrations.

## 5.2 Biological insight

In this section, we present quantitative biological insights into the relation between the biochemical parameters and the oscillation profile of protein levels in negative cyclic gene regulatory networks. In particular, we show that biological insights are easily obtained from Theorems 1 and 2, because the derived estimates are analytically written in terms of the biochemical parameters in (1).

First, we focus on the frequency of periodic oscillations. In (19),  $1/T_G$  has the physical dimension of inverse of time, and

$$\frac{-1 + \sqrt{1 + Q^2 \tan^2\left(\frac{\pi}{N}\right)}}{Q \tan\left(\frac{\pi}{N}\right)} \quad (32)$$

is dimensionless. Thus, the angular frequency of oscillations is expected as (32) when time is normalized by the geometric means of mRNA and protein time constants  $T_G = \sqrt{T_a T_b}$ .

In addition, (32) implies that  $N$ , the number of genes involved in the cyclic gene regulatory networks, and  $Q$ , the ratio between arithmetic and geometric means of mRNA and protein levels defined in (10), are the two dominant biological quantities that determine the frequency of oscillatory protein levels. Specifically, we can predict the nature of periodic oscillations by (32) as follows.

- (A) As  $Q$  gets larger, the frequency of oscillations is expected to become larger.

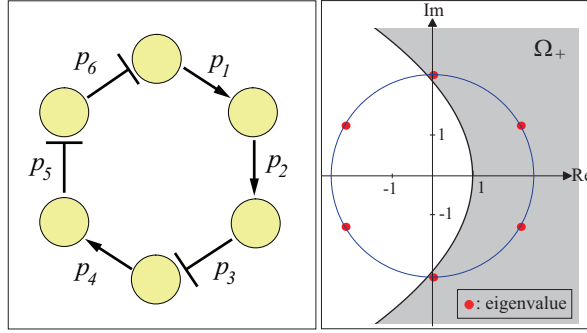


Figure 8: (Left) network motif of the considered negative cyclic gene regulatory network, (Right) graphical criterion for the existence of periodic oscillations (Proposition 1). Four eigenvalues lie inside the region  $\Omega_+$ .

(B) As the number of genes  $N$  gets larger, the frequency of oscillations is expected to become smaller.

In fact, the numerical simulation result in Fig. 7, where estimated and actual frequency of oscillations are plotted for  $N = 3, 7$  and 11 genes with  $T_G = 1$ , is consistent with the above statement. Note that  $Q$  defined by (10) satisfies  $0 < Q \leq 1$ , and the statement (A) above means that the frequency of oscillations is expected to become large when the degradation time constants of mRNA and protein, or  $T_a$  and  $T_b$ , are close to each other. Thus, from a synthetic biological viewpoint, it may be possible to obtain a desired frequency of oscillations by arranging the DNA sequence so that the resulting mRNA and protein have prescribed degradation rates.

Regarding the phase shift of oscillations between proteins, we see from Theorem 2 that the kinetic parameters in (1) are less important, but rather the network motif of activation and repression is dominant. It can be summarized as follows.

(C) The phase shift of oscillations is expected  $-\pi/N$  (phase lag) when transcription is activated, and  $1 - \pi/N$  (phase lead) when repressed.

This observation may help generate an oscillation *pattern* in negative cyclic gene regulatory networks by genetic engineering.

## 6 Discussions: Accuracy of Estimation

Since the estimated oscillation profiles in our theorems are obtained by the approximation of (11), there may be estimation errors. In this section, we discuss the accuracy of our estimation, and give a criterion to measure the accuracy of the estimated values.

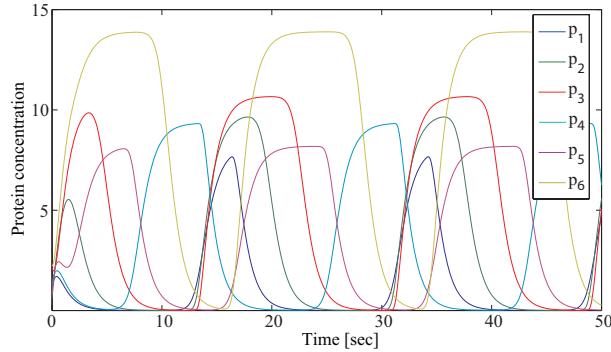


Figure 9: Time plot of oscillatory protein concentrations ( $(\prod_{i=1}^6 R_i^2)^{1/6} = 9.87$ ).

We first show an example where our results show relatively large errors. Consider the cyclic gene regulatory network depicted in Fig. 8(Left), which is the same network motif as the one in Section 5.1. Suppose all the parameters except  $c_i$  and  $\beta_i$  ( $i = 1, 2, \dots, N$ ) are identical to the ones in Section 5.1.  $c_i$  and  $\beta_i$  are given as  $c_1 = c_3 = c_5 = 6.3, c_2 = 5.8, c_4 = c_6 = 5.5$  and  $\beta_1 = \beta_5 = 3.9, \beta_2 = \beta_3 = \beta_4 = 5.1, \beta_7 = 7.6$ . Then, the estimated frequency of periodic oscillations in this cyclic gene regulatory network is obtained from (19) as  $0.409[\text{rad/s}]$ , and the actual frequency is obtained by numerical simulation as  $0.353 [\text{rad/s}]$ . The relative error is 15.9%, and the estimated period of oscillations have relatively large error compared to the example in Section 5.1.

On the other hand, the estimated and actual phase of oscillations are obtained as follows.

Protein	$p_2$	$p_3$	$p_4$	$p_5$	$p_6$
Estimated [deg]	330.0	300.0	90.0	60.0	210.0
Actual [deg]	333.7	301.3	89.0	60.7	206.3

The authors have observed by many numerical simulations that phase estimates are relatively reliable for a large range of parameters.

Since we have assumed (11) in our analysis, our estimates can show large errors when the actual waveform of protein levels deviate from a biased sinusoidal function of (11). It has been observed by numerical simulations that as the value of  $(\prod_i^N R_i^2)^{1/N}$  gets larger, waveform of protein levels deviates from the biased sinusoidal curve, and the estimation tends to give unreliable values (see Fig. 6 and 9). Note that  $R_i$  ( $i = 1, 2, \dots, N$ ) is defined in (5), and is one of the dominant biological quantities for determining the existence of periodic oscillations in cyclic gene regulatory networks. The above observation can be explained as follows. As  $(\prod_{i=1}^N R_i^2)^{1/N}$  gets larger, the system

tends to be more unstable, because  $(\prod_{i=1}^N R_i^2)^{1/N}$  is a part of the feedback gain. This means that flow around the unique equilibrium state becomes fast, and reaches saturation limit in a short time when  $(\prod_{i=1}^N R_i^2)^{1/N}$  is large. Therefore, we obtain rectangular-like waveform as illustrated in Fig. 9 when  $(\prod_{i=1}^N R_i^2)^{1/N}$  is large.

Based on the above observation, we here present a rough idea of an accuracy criterion for our estimated values. Recall that the graphical criterion of Proposition 1 is equivalent to the necessary and sufficient condition for instability of the unique equilibrium state. In particular, the region  $\Omega_+$  in Fig. 9 corresponds to the right half of the complex plane, and thus, we can conclude that the more the eigenvalues of  $M$  lies inside  $\Omega_+$ , the more unstable the linearized system  $\mathcal{G}(s)$  becomes. Therefore, we can summarize the criterion as follows. Consider the graphical condition for the existence of periodic oscillations of Proposition 1. Then, the expected frequency  $\varpi$  in Theorem 1 is more likely to be accurate when there are only two eigenvalues inside the region  $\Omega_+$ . In fact, the numerical example in Section 5.1 satisfies the above criterion as illustrated in Fig. 6, and has given a relatively accurate estimation of frequency.

## 7 Conclusion

We have investigated oscillation profiles of protein levels in large-scale gene regulatory networks with negative cyclic feedback. First, we have formulated the estimation problem of frequency, phase, bias and amplitude by using the idea of multivariable harmonic balance [10]. Then, expected frequency and phase of periodic oscillations have been derived by solving the harmonic balance equations. In particular, these estimates have the following features: (i) they can be applied to large-scale cyclic gene regulatory networks composed of any number of genes. (ii) they are analytically written only in terms of biochemical parameters, and thus, the relation between the parameters and oscillation profiles can be easily obtained. In fact, we have given several biological insights in Section 6. Finally, the accuracy of our estimation has been discussed, and the accuracy criterion has been presented.

**Acknowledgements:** The authors would like to thank Dr. Yoshiaki Futakata at the University of Tokyo for his helpful comments. This work is supported in part by Grant-Aid for Exploratory Research of the Ministry of Education, Culture, Sports, Science and Technology in Japan, No. 21656106.

## References

- [1] J. C. Dunlap, “Molecular bases for circadian clocks,” *Cell*, vol. 96, no. 2, pp. 271–290, 1999.
- [2] H. Hirata, S. Yoshiura, T. Ohtsuka, Y. Bessho, T. Harada, K. Yoshikawa, and R. Kageyama, “Oscillatory expression of the bhlh factor *hes1* regulated by a negative feedback loop,” *Science*, vol. 298, pp. 840–843, 2002.
- [3] C. Trané and E. W. Jacobsen, “Network structure and robustness of intracellular oscillators,” in *Proceedings of the 17th IFAC World Congress*, 2008, pp. 10989–10994.
- [4] M. B. Elowitz and S. Leibler, “A synthetic oscillatory network of transcriptional regulators,” *Nature*, vol. 403, no. 6767, pp. 335–338, 2000.
- [5] H. E. Samad, D. D. Vecchio, and M. Khammash, “Repressilators and promoters: Loop dynamics in synthetic gene networks,” in *Proceedings of American Control Conference*, 2005, pp. 4405–4410.
- [6] P. Rapp, “Analysis of biochemical phase shift oscillators by a harmonic balancing technique,” *Journal of Mathematical Biology*, vol. 25, no. 3, pp. 203–224, 1976.
- [7] B. C. Goodwin, “Oscillatory behavior in enzymatic control process,” *Advances in Enzyme Regulation*, vol. 3, pp. 318–356, 1965.
- [8] S. Pigolotti, S. Krishna, and M. H. Jensen, “Oscillation patterns in negative feedback loops,” *Proceedings of the National Academy of Sciences*, vol. 104, no. 16, pp. 6533–6537, 2007.
- [9] H. K. Khalil, *Nonlinear systems*. Prentice Hall, 2001.
- [10] T. Iwasaki, “Multivariable harmonic balance for central pattern generators,” *Automatica*, vol. 44, no. 12, pp. 3061–3069, 2008.
- [11] U. Alon, *An introduction to systems biology: Design principles of biological circuits*. Chapman & Hall/CRC, 2006.
- [12] Y. Hori, T.-H. Kim, and S. Hara, “Graphical and analytic criteria for the existence of protein level oscillations in cyclic gene regulatory networks,” in *Proceedings of the 48th Conference on Decision and Control*, 2009, pp. 3521–3526.
- [13] H. L. Smith, “Oscillations and multiple steady states in a cyclic gene model with repression,” *Journal of Mathematical Biology*, vol. 5, no. 2, pp. 169–190, 1987.
- [14] J. Mallet-Paret and H. L. Smith, “The Poincaré-Bendixson theorem for monotone cyclic feedback systems,” *Journal of Dynamics and Differential Equations*, vol. 2, no. 4, pp. 367–421, 1990.
- [15] S. Hara, T. Hayakawa, and H. Sugata, “LTI systems with generalized frequency variables: A unified framework for homogeneous multi-agent dynamical systems,” *SICE Journal of Control, Measurement and System Integration*, vol. 2, no. 5, pp. 299–306, 2009.
- [16] P. J. Davis, *Circulant Matrices*. John Wiley and Sons, 1979.

## A Proof of Lemma 1

It should be first noted that  $\mathcal{H}_\bullet(s)$  belongs to a class of linear systems with a generalized frequency variable proposed in [15]. The lemma can be obtained by almost the same proof as Proposition 5.1 in [15].

Let the imaginary poles of  $\mathcal{H}_\bullet(s)$  be defined by

$$\mathcal{I} := \{j\omega \mid |\phi(j\omega)I - K_\bullet| = 0\}. \quad (33)$$

It follows that  $\mathcal{H}_\bullet(s)$  has the imaginary poles  $\mathcal{I}$  and the rest in the open left half plane, if and only if  $|\phi(s)I - K_\bullet| \neq 0$  for all  $s \in \mathbb{C}_+ \setminus \mathcal{I}$  and  $|\phi(s)I - K_\bullet| = 0$  for all  $s \in \mathcal{I}$ . This is also equivalent to  $\phi(s) \neq \lambda$  for all  $s \in \mathbb{C}_+ \setminus \mathcal{I}$  and all  $\lambda \in \text{spec}(K_\bullet)$ , and  $\phi(s) = \lambda$  for all  $s \in \mathcal{I}$  and some  $\lambda \in \text{spec}(K_\bullet)$ . This immediately concludes Lemma 1.

## B Proof of Theorem 1

We consider the condition that at least one eigenvalue of  $K_\bullet$  lies on the curve  $\mathcal{C} := \{\phi(j\omega) \mid \omega \in \mathbb{R}\}$ , and the rest lies inside  $\Omega_+^c$ . This implies the conditions (i) and (ii) in Proposition 2 hold at the frequency  $\varpi$ , where the eigenvalue lies on the curve  $\mathcal{C}$ .

It follows from the definition that the gain  $|\phi(j\omega)|$  and the phase  $\arg(\phi(j\omega))$  monotonically increase with respect to  $\omega$ , which are the key properties to show this theorem. This implies that  $\phi(0) = 1$  is the closest point to the origin in the curve  $\mathcal{C}$ , and the distance between the origin and the curve  $\mathcal{C}$  monotonically increases as illustrated in Fig. 4.

Recall that the eigenvalues  $\{\lambda_i\}_{i=1}^N$  of the matrix  $K_1$  are located on a circle as shown in (18). Then, we can see that  $\lambda_1$  always crosses  $\mathcal{C}$  first, when the radius of the circle increases, because of the monotone property of  $\phi(j\omega)$  shown above. Thus, the problem is reduced to finding  $\varpi$  satisfying

$$\phi(j\varpi) = \lambda_1. \quad (34)$$

It follows from (34) that

$$\arg(\phi(j\varpi)) = \frac{\pi}{N}. \quad (35)$$

Let  $\theta_1 := \arctan(T_a\varpi)$  and  $\theta_2 := \arctan(T_b\varpi)$ . Then, (35) can be written as

$$\theta_1 + \theta_2 = \frac{\pi}{N}, \quad (36)$$

and this implies

$$\tan(\theta_1 + \theta_2) = \tan\left(\frac{\pi}{N}\right). \quad (37)$$

Then, (37) and the trigonometric addition formula yields

$$\frac{(T_a + T_b)\varpi}{1 - T_a T_b \varpi^2} = \tan\left(\frac{\pi}{N}\right). \quad (38)$$

The predicted frequency  $\varpi$  is obtained by clearing the fraction and applying the quadratic formula to the above equation.